Persistent Shift from Oxidative to Glycolytic Fibers Underlies Quadriceps Weakness Post-Anterior Cruciate Ligament Injury

Jian-ting LI[1], Sai-Chuen Fu[1,3], Patrick, Shu-Hang Yung[1,2,3]
[1]Department of Orthopaedics & Traumatology, Faculty of Medicine, The Chinese University of Hong Kong
[2] CUHK Medical Center, Department of Orthopaedics & Traumatology, Faculty of Medicine, The Chinese University of Hong Kong.
[3] Center for Neuromusculoskeletal Restorative Medicine Limited, Hong Kong.
gracelijianting@link.cuhk.edu.hk

Disclosures: No disclosures.

INTRODUCTION: Persistent quadriceps weakness following ACL injury remains incompletely understood. Notably, quadriceps atrophy persists bilaterally after ACL in jury and reconstruction, posing a significant barrier to full functional recovery. Although muscle mass may be restored post-rehabilitation, shifts in muscle fiber composition toward glycolytic phenotypes have been observed in the injured limb[1,2]. These changes are likely contributors to impaired muscle endurance[3] and delayed muscle reaction time[4]. Understanding the origins and timing of these fiber-type alterations is critical for developing effective treatment strategies. Given that oxidative and glycolytic fibers differ in mitochondrial content and oxidative stress is a established driver of muscle atrophy, we hypothesized that reactive oxygen species (ROS) might influence fiber-type shifts by compromising mitochondrial integrity. In this study, we employed a murine ACL rupture model to track temporal changes in quadriceps fiber composition alongside oxidative stress. C2C12 myotubes were subjected to varying concentrations of hydrogen peroxide (H_2O_2) to directly assess the role of ROS in regulating specific muscle fiber phenotypes.
METHODS: Fifteen 10-week-old male C57BL/6 mice underwent unilateral, non-invasive ACL rupture, with five uninjured mice as healthy controls. Quadriceps muscles from injured and contralateral limbs were collected at 1, 2, and 4 weeks post-injury (n = 5 per time point) and from controls, weighed to assess muscle mass, cryosectioned, and stained for Laminin (fiber cross sectional area (CSA)), MyHC isoforms (Type I, IIA, IIB fibers), and 4-hydroxynonenal (4-HNE, oxidative damage). In vitro, C2C12 myoblasts were differentiated into myotubes for four days and treated with 0, 50, 100, or 200 µM H_2O_2; mitochondrial content (MitoTracker), mitochondrial membrane potential (JC-1), and mitochondrial ROS (MitoSOX) were measured at 4 hours, and MyHC RNA and protein expression were assessed at 24 hours by qPCR and Western blot. All procedures adhered to institutional animal ethics guidelines. Data are presented as mean ± SEM; two-way ANOVA with Bonferroni's post hoc test assessed muscle and MyHC outcomes, one-way ANOVA evaluated mitochondrial parameters, and $P < 0.05$ is considered significant.
RESULTS SECTION: Muscle mass in both injured and contralateral limbs declined during the first two weeks and recovered by week 4(**Figure 1A**). Oxidative type I fiber was not detected in the quadriceps sections. In injured limbs, oxidative Type IIA fibers were markedly atrophied at week 1 ($p = 0.003$) and week 2 ($p = 0.002$) and remained smaller than healthy controls at week 4 ($p = 0.03$) (**Figure 1B, C**). In contrast, glycolytic (Type IIB) fibers only transiently shrank at week 2 ($p = 0.05$) and recovered by week 4 ($p = 0.89$) (**Figure 1B, C**). Contralateral limbs showed no significant changes in either fiber type relative to healthy controls. The oxidative-to-glycolytic CSA ratio was reduced at week 1 ($p = 0.002$), week 2 ($p = 0.001$), and remained low at week 4 ($p = 0.005$). Similarly, the oxidative-to-glycolytic fiber count ratio was significantly lower at weeks 1, 2, and 4 compared with controls ($p < 0.001$ for all) (**Figure 1C**). Despite restored muscle mass, oxidative damage accumulated progressively, with ~15-fold and ~2.5-fold increases in 4-HNE staining in injured ($p = 0.001$) and contralateral limbs ($p = 0.08$), respectively (**Figure 2**). In vitro, 200 µM H_2O_2 induced a shift toward glycolytic myosin heavy chain expression, while 50 µM uniquely upregulated Myh2 (oxidative) mRNA ($p < 0.001$), but the protein levels remained unchanged (**Figure 3A-C**). C2C12 myotubes treated with 100 µM and 200 µM H_2O_2 for 4 hours exhibited dose-dependent increases in mitochondrial ROS generation (0 vs. 100 µM: $p = 0.03$; 0 vs. 200 µM: $p = 0.004$) and decreases in membrane potential (0 vs. 100 µM: $p = 0.04$; 0 vs. 200 µM: $p = 0.003$) (**Figure 3 D, F, G**), along with significant reductions in mitochondrial density (0 vs. 100 µM: $p < 0.001$; 0 vs. 200 µM: $p < 0.001$), whereas 50 µM H_2O_2 had no effect ($p > 0.99$ and $p = 0.53$) (**Figure 3 D, E**).
DISCUSSION: Our findings demonstrate that quadriceps fiber composition shifts from oxidative to glycolytic phenotypes during the early atrophic phase and remains altered even after muscle mass has recovered. In vitro, increased ROS concentrations were shown to compromise mitochondrial integrity and drive a shift toward glycolytic fiber phenotypes. The persistent atrophy of Type IIA fibers, despite recovery of Type IIB fiber size, suggests that oxidative fibers are particularly susceptible to sustained oxidative stress, likely due to their higher mitochondrial content, which impedes restoration of the pre-injury fiber distribution. These dose-dependent effects highlight mitochondrial homeostasis as a regulator of muscle fiber plasticity following injury. However, the mechanisms driving progressive oxidative damage in both injured and contralateral quadriceps remain unclear, as does the specific role of mitochondria in mediating fiber-type shifts after ACL injury. Further studies are needed to elucidate these alterations.
SIGNIFICANCE/CLINICAL RELEVANCE: The early and sustained shift to glycolytic fiber phenotypes in injured quadriceps, together with progressive oxidative damage in both injured and contralateral limbs following ACL rupture, likely underlie persistent muscle weakness. Therapeutic and rehabilitative interventions that preserve oxidative fibers and attenuate oxidative damage may reduce long-term functional impairments.
References: 1. Brain Noehren, et al. J Bone Joint Surg Am. (2016), 2. Christine M.L et al. Free Radic Biol Med. (2024), 3. Lee DH et al. Arthroscopy. (2015), 4. Tourville TW et al. J Orthop Res. (2022).

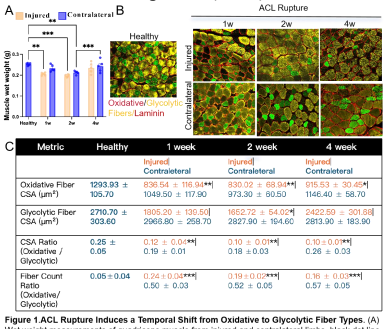

C	Metric	Healthy	1 week	2 week	4 week
			Injured / Contralateral	Injured / Contralateral	Injured / Contralateral
	Oxidative Fiber CSA (µm²)	1293.93 ± 105.70	836.54 ± 116.94** / 1049.50 ± 117.90	830.02 ± 68.94** / 973.30 ± 60.50	915.53 ± 30.45* / 1146.40 ± 58.70
	Glycolytic Fiber CSA (µm²)	2710.70 ± 303.60	1905.20 ± 130.50 / 2966.80 ± 259.70	1652.72 ± 54.02* / 2827.90 ± 164.60	2422.59 ± 201.88 / 2813.90 ± 183.90
	CSA Ratio (Oxidative / Glycolytic)	0.25 ± 0.05	0.12 ± 0.04** / 0.19 ± 0.01	0.10 ± 0.01** / 0.18 ± 0.03	0.10 ± 0.01** / 0.26 ± 0.03
	Fiber Count Ratio (Oxidative/ Glycolytic)	0.05 ± 0.04	0.24 ± 0.04*** / 0.50 ± 0.03	0.19 ± 0.02*** / 0.52 ± 0.05	0.16 ± 0.03*** / 0.57 ± 0.05

Figure 1.ACL Rupture Induces a Temporal Shift from Oxidative to Glycolytic Fiber Types. (A) Wet weight measurements of quadriceps muscle from injured and contralateral limbs, black dot line indicated the muscle weight range of healthy mice. (B) Representative immunohistochemical staining for muscle fiber types in quadriceps from healthy and ACL-injured limbs at 1, 2, and 4 weeks post-injury. (C) Quantification of median CSA for specific fiber types, along with the ratio of oxidative to glycolytic fiber area and count. Scale bar, 200 µm. *p < 0.05, **p < 0.01, ***p < 0.005 compared to healthy controls.

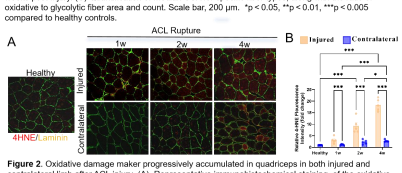

Figure 2. Oxidative damage maker progressively accumulated in quadriceps in both injured and contralateral limb after ACL injury. (A) Representative immunohistochemical staining of the oxidative damagemarker 4-HNE. (B) Quantification of 4-HNE staining in quadriceps from healthy and ACL-injured mice across time points. Scale bar, 200 µm. *p < 0.05, ***p < 0.005 compared to healthy controls.

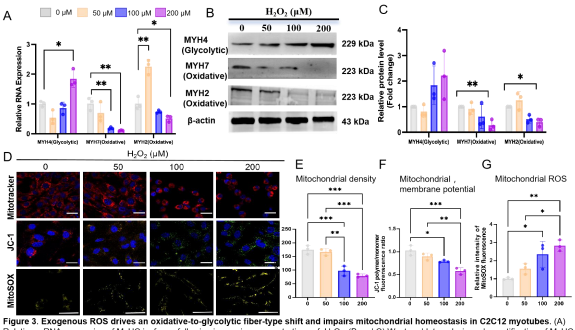

Figure 3. Exogenous ROS drives an oxidative-to-glycolytic fiber-type shift and impairs mitochondrial homeostasis in C2C12 myotubes. (A) Relative mRNA expression of MyHC isoforms following increasing concentrations of H_2O_2; (B and C) Western blot analysis and quantification of MyHC isoform proteins normalized to β-actin after H_2O_2 treatment ; (D) Representative fluorescence images of mitochondria (Mitotracker), mitochondrial membrane potential (JC-1), and mitochondrial ROS (MitoSOX) in treated myotubes; scale bars: 25 µm (Mitotracker, JC-1), 100 µm (MitoSOX). (E, F, and G) Quantification of mitochondrial density, mitochondrial membrane potential via JC-1 red/green fluorescence ratio., and mitochondrial ROS by MitoSOX fluorescence intensity. n = 3 per group. *p < 0.05, **p < 0.01, ***p < 0.005.